AFRL-AFOSR-JP-TR-2023-0044

Q-Bits on Assembled Hybrid Materials
(Molecular Design of Organically Modified Qubits ?)

Eunkyoung Kim
YONSEI UNIVERSITY UNIVERSITY-INDUSTRY FOUNDATION
50 YONSEI-RO, SEODAEMUN-GU
SEOUL, SEOUL, 03722
KOR

11/19/2022
Final Technical Report

Air Force Research Laboratory
Air Force Office of Scientific Research
Asian Office of Aerospace Research and Development
Unit 45002, APO AP 96338-5002

REPORT DOCUMENTATION PAGE

PLEASE DO NOT RETURN YOUR FORM TO THE ABOVE ORGANIZATION.

1. REPORT DATE	**2. REPORT TYPE**	**3. DATES COVERED**	
20221119	Final	**START DATE** 20190904	**END DATE** 20200903

4. TITLE AND SUBTITLE
Q-Bits on Assembled Hybrid Materials
(Molecular Design of Organically Modified Qubits ?)

5a. CONTRACT NUMBER	**5b. GRANT NUMBER**	**5c. PROGRAM ELEMENT NUMBER**
FA2386-19-1-4070		61102F
5d. PROJECT NUMBER	**5e. TASK NUMBER**	**5f. WORK UNIT NUMBER**

6. AUTHOR(S)
Eunkyoung Kim

7. PERFORMING ORGANIZATION NAME(S) AND ADDRESS(ES)
YONSEI UNIVERSITY UNIVERSITY-INDUSTRY FOUNDATION
50 YONSEI-RO, SEODAEMUN-GU
SEOUL, SEOUL 03722
KOR

8. PERFORMING ORGANIZATION REPORT NUMBER

9. SPONSORING/MONITORING AGENCY NAME(S) AND ADDRESS(ES)	**10. SPONSOR/MONITOR'S ACRONYM(S)**	**11. SPONSOR/MONITOR'S REPORT NUMBER(S)**
AOARD UNIT 45002 APO AP 96338-5002	AFRL/AFOSR IOA	AFRL-AFOSR-JP-TR-2023-0044

12. DISTRIBUTION/AVAILABILITY STATEMENT
A Distribution Unlimited: PB Public Release

13. SUPPLEMENTARY NOTES

14. ABSTRACT
Organically modified qubits (OMQs) were designed to pertain ordered arrangement of spins and provide controllability on electronic spin states in qubits via external stimuli. OMQs with three
different structural groups were synthesized: 1) metalophthalocyanines with different ligands 2) luminescent organic radicals (LORs), and 3) conjugated polymer magnets. These OMQs were
oriented vertically on a 2D surface, to modulate the electronic properties of the surface against the spin direction. The ligand on the metalophthalocyanines was critical to achieve a large
magneto resistance ratio (MR). Thus a thioalkyl ligand of the Tb(Pc2)(SR8) showed the highest MR at room temperature, indicating that it could provide high tunability in electron spins.

15. SUBJECT TERMS

16. SECURITY CLASSIFICATION OF:			**17. LIMITATION OF ABSTRACT**	**18. NUMBER OF PAGES**
a. REPORT	**b. ABSTRACT**	**c. THIS PAGE**		
U	U	U	SAR	21

19a. NAME OF RESPONSIBLE PERSON	**19b. PHONE NUMBER** *(Include area code)*
TONY KIM	315-227-7008

AOARD Project Final Report
(September, 04, 2019 – September, 03, 2020)

Grant: FA9550-19-S-0003

Molecular System for Organically Modified Qubits

December 3, 2020

Key Researcher (PI):

Prof. Eunkyoung Kim
Institution: Department of Chemical and Biomolecular Engineering, Yonsei University
Mailing address: 50 Yonsei-ro, Seodaemun-gu, Seoul, 03722, South Korea
Phone: +82-2-2123-5752, FAX: +82-2-2123-8600
E-mail address: eunkim@yonsei.ac.kr

Joint Researchers

Prof. Kwang-Sup Lee
Institution: Department of Advanced Materials, Hannam University
Mailing address: 461-6 Jeonmin-Dong, Yuseong-Gu, Daejeon 305-811, South Korea
Phone: +82-42-629-8857, FAX: +82-42-629-8854
E-mail address: kslee@hannam.ac.kr

AFOSR Program Manager Dr. Tony Kim

Abstract
Organically modified qubits (**OMQs**) were designed to pertain ordered arrangement of spins and provide controllability on electronic spin states in qubits via external stimuli. OMQs with three different structural groups were synthesized: 1) metalophthalocyanines with different ligands 2) luminescent organic radicals (**LORs**), and 3) conjugated polymer magnets. These OMQs were oriented vertically on a 2D surface, to modulate the electronic properties of the surface against the spin direction. The ligand on the metalophthalocyanines was critical to achieve a large magneto resistance ratio (MR). Thus a thioalkyl ligand of the $Tb(Pc_2)(SR_8)$ showed the highest MR at room temperature, indicating that it could provide high tunability in electron spins. The end-on structured LORs showed large MR, which is much larger than those of the reported materials. The end-on oriented PEDOTs on graphene showed a high degree of crystallinity and free-electron-like charge transport properties with an enhanced Hall mobility, which allowed modulation of TE properties via external stimuli. Taking advantage of graphene functionality, thermoelectric properties were largely modulated *via* external magnetic field as a giant magneto-thermoelectric effect of ~-73.6% and Seebeck coefficient of -49% at 298 K. This result provides a unique tool for a multifunctional electron spintronics. In these OMQs at the molecular level, the origin of the magnetism could be from both orbital and spin angular momentums of a molecule or polymer rod, which is placed in a ligand field. Thus further research on robust qubits based on OMQs could establish the optimum spin-orbit coupling and their electro-optical teleportation.

1. Introduction

A need to shift in computer technology is fast approaching because of the limitation in the frequency (bandwidth) of silicon electronics and printed metallic tracks. Since quantum states of spins in solids or in molecules are tunable and coherently manipulated by means of external electromagnetic fields, spins provide a simple platform to encode a quantum bit (qubit). Thus quantum coherence sits at the heart of quantum information processing (**QIP**), in which coherence between two or more quantum mechanical systems is a key to create quantum-bits (**qubits**).

For a long time, many research groups were in pursuit of quantum supremacy, which may demonstrate a programmable quantum computing that can solve a problem that no classical computer can solve in any feasible amount of time. This goal was achieved in part in 2019 by the quantum computing team at Google[1]. However, the concept of quantum supremacy itself was challenged in 2020[2], and alternatively a term called quantum advantage was mooted[3]. The number of qubits in a quantum computer has dramatically changed in the last decade. Recently, Neven's Law, analogous to Moore's law for conventional computers, has been defined for the number of qubits in a quantum computer (QC). Neven's Law states that the number of Q-bits scales by a double exponential every two years[4].

The working principle and magnetic behaviour to achieve qubits are based on the ability to generate and control quantum superpositions of two basis states ('0' and '1') and to read out the outcome. Because quantum superpositions are often fragile and quickly erased by noise (for eg. phonons, electric or magnetic noise), the coherence is lost. Such *decoherence* is a major obstacle for the development of solid-state quantum technologies[5,6]. To maximize quantum coherence, it

is necessary to design the electronic structure of the spin qubit and its atomic environment in a molecular approach. In particular, electronic spins are prime candidates as qubits since microwave pulses can be used to create and manipulate superpositions of pairs of spin orientation, which ultimately may provide switchable channels between two different molecular units. A promising chemical approach to creating qubits utilizes molecular electronic spin levels in inorganic complexes[5]. The versatility of inorganic complex synthesis allows chemical tunability of properties to suit qubit applications. The interaction between inorganic complex molecules can be synthetically tuned to define the interaction between qubits possibly towards achieving large matrices of interactive qubits. Further they hold the promise of being able to generate electronic spin-nuclear spin mixed based qubits. Such qubits can lead to longer coherence times compared to pure electronic spin qubits.

In this context, this project puts forward chemical strategies to assemble qubits from organic-inorganic hybrid materials. Herein we focused on the synthesis of hybrid material assembly for organically modified qubits (**OMQs**), characterization of their electro-optic properties, and possibility of generating parallel qubits from them. As a new material platform, we focus on metalophthalocyanine quibits modified with pi-conjugated ligands (**MPCQ**), to achieve long quantum coherence, programmable under quantum operations, and scalable to a large number of qubits. Further non-covalently tethered qubits based on assembled spin systems on a graphene matrix (**NCTQ**) will be investigated.

Intense research into 2D materials have evolved a wealth of strategies for massive non-covalent assemblies on molecules onto 2D materials. Thus specific ligands on a magnetic molecule were designed to tether OQMs on graphene 2D surface at one end and complex with an OQM hosting the spin qubit. To go beyond the optimization of molecular structure, we explore a method to integrate the molecular quantum units by solution processing of the molecule and explore the controllability of magnetic properties of OQMs by electrical, optical, and thermal stimuli. In this context, OQMs with three different structural groups were designed" 1) metalophthalocyanines with different ligands 2) luminescent organic radicals (**LORs**), and 3) conjugated polymer magnets.. The electronic states of 2D materials are surface state. Thus it is possible to create decoupled monolayer or stacked molecular spin structure on 2 D surface. A solution process for these materials was explored to arrange those OQMs on a 2D surface, which could provide a molecular spin system that can be coherently controlled via external electromagnetic fields. Their discrete electronic states and switchability of the spins states were examined by PPMS and Hall measurement along with their electrooptical characterization. As the end on structure of organic radicals and conjugated polymer spins were designed to pertain electrochemical activity, their magnetic resistance and carrier density were controlled by external voltage. Furthermore the organic radicals were designed to covalently connected to a luminescent group, to provide possibility of spin orbital coupling through intersystem conversion that are crucial for photodriven quantum teleportation of an electron spin state in these system.

Non-covalent self-assembly of polyaromatic molecules on graphene allows the generation of precise arrays of molecules and materials[7]. The highly selective and specific interaction between polyaromatic moieties and graphene surface could be exploited to achieve a highly ordered arrangement of qubits. The design of the ligand involves a polyaromatic tethering group at one end and a functional group or moiety capable of ligating to nanoparticles or metal ions on the other end. Two different ligands, L1 and L2, have been designed in this theme. The first ligand

L1 has OH-groups as the ligating moiety and the second one (L2) has bitholane group as the ligating group. Such ligands have been used in the past to make molecular-level assemblies of non-covalent molecules on graphene surfaces. The pi-pi interactions between the polyaromatic tethers and other two-dimensional materials can be further used for extending the search of Q-bits for two-dimensional materials in general. Vanadium (IV) complexes are a good system to study such interactions. Some recent investigations in vanadium complexes have revealed results on par with solid state qubits currently being applied in quantum computers[8]. The results of synthesis and assembly of nanohybrid structures for QIP are discussed in the following sections.

Using these molecular spin systems, we illustrate the effect of structure on magnetic sensitivity and propose design principles and processing methods of molecular spin qubits. Putting all together we synthesized the following structures (Figure 1). The first structure is based on $Tb(Pc)_2$, in which organic groups are introduced as a side group. In the 2nd structure, an organic radical is linked to a luminescent unit, to pertain their optical properties along with spins. These radicals were further modified with a linker that bound to inorganic 2D surface and metalophthalocyanine unit to explore possibility of orthogonal control of their spin properties against optical and electrical stimuli. Third structure is designed for polaron radials based on conjugated polymers. In the last example, we used a self-assembled host of a phthalocyanine derivative on graphene and a conjugated molecule as a guest. These molecules are never synthesized thus it provides a new family of organic spins.

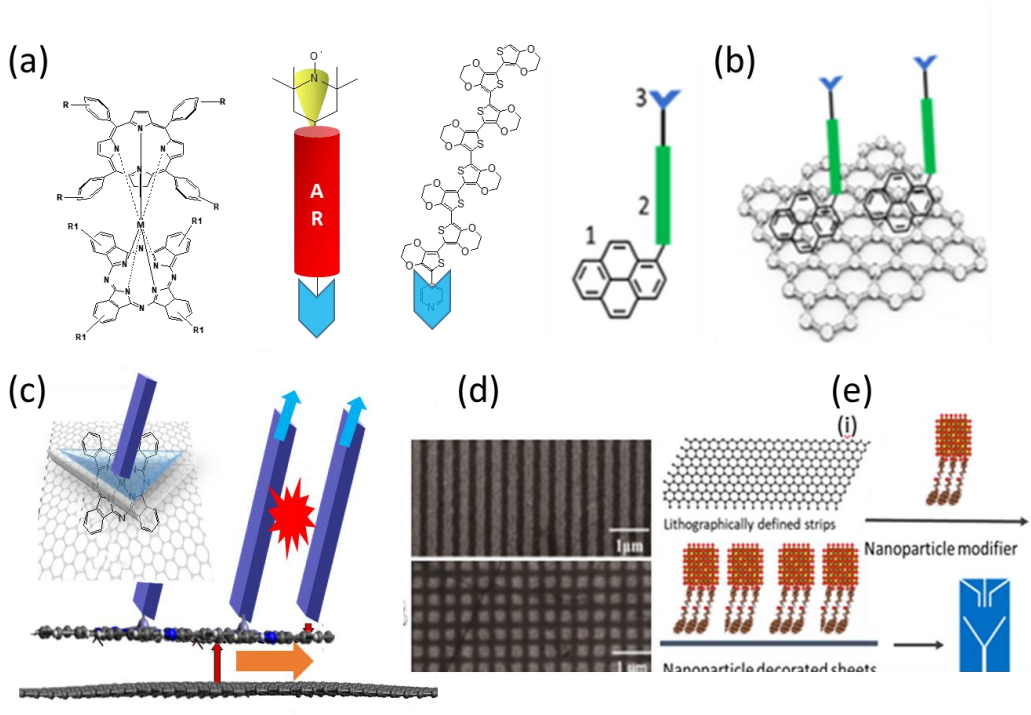

Figure 1. (a) Proposed structures for new qubit materials based on organically modified qubits. (b) and (c) Molecular arrangement on a 2 D surface. (d) and (e) Processes for device fabrication of qubits.

2. Experiment

2.1. Materials

All the reagents used in this study were purchased from Sigma Aldrich of TCI chemicals unless described specifically. Tributylamine (99%) was purchased from ACROS product. Deionized water was purchased from Duksan general science. Other materials were used without further purification. Highly oriented pyrolytic graphite (HOPG, ZYB, 15 mm × 15 mm × 2 mm) was purchased from MaTecK, GmbH. Monolayer graphene grown by CVD processing onto copper foil, and that then transferred onto quartz (1" × 1") or poly(ethylene terephthalate) (PET) film (1" × 1") was purchased from Graphene Supermarket. A 250 μm Pt/Ir (90/10) wire purchased from Goodfellow was mechanically cut to fabricate a tip prior to use for STM measurement. Graphene used for ***vanadium complex*** were purchased from prepared by the electrochemical exfoliation method described by Müllen et. al[9].

2.1.1. Synthesis of metalophthalocyanines with pi-conjugaed ligands (MPCQ).

To obtain the materials for qubits we synthesized metalophthalocyanines containing a Tb or Ln ion, as an f-block metal. Three different $Tb(Pc)_2(R)_8$ were synthesized from unsubstituted (R=H) or disubstituted (R) 1,2-dicyanobenzene with $Tb^{3+}(acac)_3{\cdot}4H_2O$ in alcohol at elevated temperature, where the side chain (R) is H, O-alkyl, and S-alkyl groups. Similarly blue (anionic $[LnPc_2]^-$) and green (neutral $[LnPc_2]^0$), were obtained. The unstable anionic form was converted to the stable neutral form. Thus a mixture of 1,2-dicyanobenzene (42mmol), $Tb^{3+}(acac)_3{\cdot}4H_2O$ (5mmol), DBU (21mmol) were dissolved in 50mL of 1-pentanol and refluxed for 1.5days. The solution was allowed to cool to room temperature and then acetic acid was added. The mixture was heated at 100℃. After 0.5h stirring, the mixture was cooled and the precipitates were collected by filtration. The product was washed and purified using a solvent mixture. Both forms, blue (anionic $[LnPc_2]^-$) and green (neutral $[LnPc_2]^0$), were obtained simultaneously, as revealed by electronic absorption spectra. In order to convert the unstabilized anionic form to the neutral one, the reaction mixture was presorbed on active (H_2O-0%) basic alumina oxide. Purification was carried out by column chromatography on basic alumina oxide (deactivated with 4.6% H_2O, level IV) with chloroform-methanol mixture (10:1) as eluent. In general, the yield was 30-35%.

2.1.2. Synthesis of TEMPO substituted fluorene with pyridine linker (TFlPy).

To a solution of bromofluorenic acid (1 eq) in 30 mL of dry THF, dmap (0.1 eq) wa added. Then, DCC (1.1 eq) was added and let stirred for 30 minutes. 4-HydroxyTEMPO 160mg(1.2eq), were added and the reaction mixture was stirred for 24 h at room temperature. After 1 day, Add DMAP 19.2mg(0.2eq) for completing the reaction. The concentrated product was loaded onto a silica gel column and the product was separated by column chromatography using a mixture of hexane:EtOAc to give *TFlPy* yellow solids. LC-MS : [(M+1+H+)] = m/z : 444.115.

2.1.3. Synthesis of TEMPO substituted fluorene with bromo linker (TFlBr).

To a solution of TEMPO substituted fluorenic acid (1 eq) in 30 mL of dry THF, dmap (0.1 eq)was added. Then, DCC (1.1 eq) was added and let stirred for 30 minutes. 4-HydroxyTEMPO

(1.2eq) was added and the reaction mixture was stirred for 24 h at room temperature. After the reaction, the concentrated product mixture was loaded onto a silica gel column and the product was separated by column chromatography using a mixture of hexane:EtOAc, to give TFlBr as yellow solids. LC-MS : [M+H+] = m/z : 442.2249.

2.1.4. Synthesis of TEMPO substituted benzothiazol with pyridine linker (TBtPy)

4-Hydroxy TEMPO (1 mmol) was dissolved in anhydrous acetone and stirred at room temperature. After 30 minutes of stirring, sodium hydride (60 % in mineral oil, 1.5 mmol), and was added. After 10 min of stirring, a solution of pyridine substitutend benzothiazol (1 mmol) in anhydrous acetone (10 mL) were added to the solution. The reaction mixture was stirred at room temperature. After 12 hours solvent was removed and the product mixture was diluted in dichloromethane, then washed with DI water. After removing solvents, the crude products were purified by column chromatography with hexane and dichlroromethane (hexane : DCM = 1:1) to give TBtPy as yellow solids.

2.1.5. Synthesis of pyridine substituted monomer (EDOT-Py, 2) for ordered electroactive magnetic polymer chain

4-Pyridylboronic acid pinacol ester (1.3 g, 6.3 mmol, 1.4 equiv.), tetrakis(triphenylphosphine) palladium(0) (0.52 g, 0.45 mmol, 0.1 equiv.), potassium phosphate (2.88 g, 13.6 mmol, 3 equiv.) were added into a 50 mL two-necked flask. Under argon atmosphere, 1,4-dioxane (20 mL) and the crude liquid of 2-bromo-EDOT (1.0 g) were added, and the mixture was stirred for 72 h at 90 °C. After cooling down to room temperature, the residue was filtered and washed with chloroform. The filtrate was evaporated to give a dark brown residue, which was further purified by silica gel column chromatography using a mixture of chloroform and methanol (500:1 to 500:20 gradient) to give the product as a brown powder (200 mg, 20%). Di-EDOT-pyridyl and EDOT-di-pyridyl compounds were present in the dark brown crude confirmed by NMR. ^{1}H NMR (400 MHz, $CDCl_3$, δ) 8.55 (s, Py-2H and Py-6H, 2H), 7.60 (d, J = 4.3 Hz, Py-3H and Py-5H, ~1.3H), 7.51 (d, J = 4.4 Hz, Py-5H and Py-3H, ~0.7H), 6.45 (s, Th-H, 1H), 4.38−4.36 (m, -O-CH_2-C-, 2H), 4.28−4.26 (m, -O-CH_2-C-, 2H).

2.1.6. Synthesis of hydroxyl ligand (L1)

To synthesize L1, 1-pyrenebutyric acid (1.5 g, 5.2 mmol) was reacted with pentafluoro phenyl trifluoroacetate at room temperature in 70 mL DMF solvent in the presence of triethylamine for 8 hr. At the end of the reaction, DCM was added to the reaction mixture followed by solvent separation with brine and dried over $MgSO_4$. The organic phase on removing solvents gave a dirty white solid which was purified by column chromatography to obtain the pentafluorphenyl ester of pyrene butanoic acid. ^{19}F-NMR: 164.4 (dd, 2F), 159.9 (t, 1F), 155.3 (d, 2F). The purified product was stirred with dopamine hydrochloride in DMF solvent in the presence of triethylamine at room temperature for 10 hr. The reaction mixture was washed with DCM and brine. The organic phase on removing solvents gave a dirty yellow oil (L1) which was purified by filtering after washing. ^{1}H-NMR (400 MHz, DMSO, δ): 8.39-8.37 (d, 1H), 8.29-8.21 multiple peaks (5H), 8.16-8.11 (q, 3H), 8.08-8.04 (t, 1H), 7.94-7.92 (d, 1H), 7.88-7.86 (t, 1H), 6.63-6.58 (m, 3H), 6.45-6.43 (dd, 1H), 3.23-3.19 (q, 2H), 2.55-2.53 (d, 3H), 2.24-2.20 (t, 2H), 2.04-1.97(qui, 2H).

2.1.7. Synthesis of bitholane ligand (L2)

To synthesize L2 under nitrogen flow, pyrenemethanol (0.32g, 1.4 mmol) was dissolved in 70mL DCM. α-Lipoic acid (0.346 g, 1.68 mmol) and DMAP (0.513g, 4.2 mmol) were then added at room temperature. After cooling at 0℃, a solution of DCC (0.3466 g, 1.68 mmol) in dichloromethane (28 mL) was added dropwise for 1 hr. L-Cysteine (0.5%) was added to the solution as a polymerization inhibitor. The reaction was kept at room temperature for 24 hr. At the end, the mixture was filtered. Following evaporation of the solvent under vacuum, the residue was solubilized with ethyl acetate and treated with a solution of 1N HCl. The aqueous phase was extracted with ethyl acetate. The organic phase was washed with saturated solution of NaCl and dried over $MgSO_4$. The reaction mixture (L2) was purified by chromatography on silica gel.

2.1.8. Synthesis of vanadium complex (VL1)

To synthesize VL1, under nitrogen flow $VO(acac)_2$ (0.11 g, 0.421 mmol) was reacted with L1 (0.5 g, 1.180 mmol) at room temperature in 6 mL THF. A solution of 200 μL (0.841 mmol) n-Bu_3N was added to the mixture with gentle shaking, resulting almost immediately in an intensely dark blue solution. The reaction mixture was stirred overnight. All volatile materials were removed under reduced pressure. The resulting dark blue residue was washed twice 5 mL cold diethyl ether and twice 5 mL hexane and then was dried under reduced pressure to yield 0.8 g of dark blue powder (***VL1)***.

2.2. Preparation of the PEDOT:Tos films

PEDOT:Tos films were prepared using solution casting polymerization (SCP) method with slight modifications following the previous reports.[10,11] PEPG (0.20 g) was added to the oxidative solution (1.0 g, 40 wt% of iron(III) *p*-toluenesulfonate in n-butanol) and stirred for 3 h. Pyridine (13.5 mg) was added to the solution and stirred for 20 min. Then, a homogeneous red solution was obtained by filtration using a hydrophilic syringe filter (0.45 μm) and EDOT (44.1 mg) was added prior to use. The molar composition of the mixture was monomer:iron(III) *p*-toluenesulfonate:pyridine= 1:10.5:0.31. The self-assembled EDOT-Py treated substrates were used without additional process after preparing as above. But, PET films (2.5×2.5 cm^2), glass slides (2.5×2.5 cm^2), or quartz (1.0×1.0 cm^2) were treated with O_2 plasma for 3 min with a flow rate of 40.0 sccm prior to use (Cute, Femto Science Inc.). Then, the monomeric solution (16 μL cm^{-2}) was spin-coated onto the substrates using various spin speeds (1500−8000 rpm) for 30 s to control the thickness of the polymer films and heated at 60 °C and 35% RH. After 10 min, the polymer films were washed two times with ethanol to remove the used catalyst, residual oxidant, and impurities. Finally, the polymer films were dried under N_2 flow and annealed at 60 °C for 5 min.

2.3. Non-covalent coupling of VL1 with graphene (GVL1)

The ligand was coupled for graphene with simple ultrasonication experiments which were carried out under room temperature. In a typical experiment 3 ml of 1 mg/ml dispersion of graphene in nitrogenated NMP was taken in a vial equipped with a rubber septum. The complex VL1 was dissolved in 1:1 THF-NMP mixture, 3 ml (1 mg/ml) and injected directly into the graphene dispersion. The combined mixture was sonicated for 30 min (RT). After reaction, the reactant mixture was centrifuged (4000 rpm), and the supernatant was discarded. The centrifugate was shaken with THF to dissolve any excess VL1 ligands. Followed by further centrifugation to

precipitate GVL1. The THF washing was repeated 2 more times and the final centrifugate was redissolved in THF: NMP (1:1) solvent. Another reaction was carried out with the same procedure but varying the concentration of VL1 (3 ml, 5 mg/ml).

2.4. Characterization

The progress of the synthesis process of the intermediate and final material synthesized in this study was confirmed by TLC (silica gel 60F254), and column chromatography was separated using silica gel 60 (70-230 mesh) manufactured by Merck. The synthesized ligands were confirmed their structures by using the Bruker AVANCE III HD 400MHz Fourier Transform-Nuclear Magnetic Resonance (NMR), and the chemical mobility was measured using dimethylsulfide (DMSO, 2.50 ppm) containing the internal standard, tetramethylsilane (TSM). Fourier Transform Infrared spectroscopy (FT-IR) used Simadzu's IR Affinity-1S to confirm the functional groups of the material. Ultraviolet-visible spectroscopy (UV-vis) measured the absorbance and the band gap of the material using UV-3600 manufactured by Shimadzu over the range 250−800 nm. Photoluminescence (PL) spectra were obtained using a Scinco FluoroMate FS-2 at excitation wavelength of 325 nm to obtain the fluorescence wavelength position, intensity, and full width at half maximum (FWHM) of the material. UV-vis-NIR spectra for PEDOTs and LORs were performed on a UV/Vis/NIR Spectrophotometer (Lambda 750, PerkinElmer). The resistance (R) of the films was measured using a potentiostat and a four-point probe (Macor probe, 1.00 mm probe spacing, 200 μm tip radius, 100 g loads, Jandel, UK). The thickness (t) of the films was measured using an Alpha step profilometer (Tencor Instruments, Alpha-step IQ) with an accuracy of 1 nm. Also, the t was confirmed by line profiles of atomic force microscopy (AFM, NX-10, ParkSystems). The σ, charge carrier concentration, carrier mobility, and Hall coefficient were measured using an HMS-5300 Hall measurement system (Ecopia) with a magnetic field of 0.53 T from 80 to 308 K. For thermoelectric measurement, the synchronized Seebeck voltage and temperature gradient measured by two T-type thermocouples were obtained using a homemade shielded setup and the temperature gradient was confirmed by a high-resolution IR camera (FLIR E40). [10,11] Six points for ΔT and ΔV were obtained 3 times for each sample and linearly fitted to calculate the Seebeck coefficient. The parallel Au electrodes were thermally evaporated on a graphene substrate with a thickness of 100 nm.

2.5. Measurement of magnetoresistance.

The transverse resistance of the film was measured using an HMS-5300 Hall measurement system (Ecopia) at external magnetic field (0.53 T) applied perpendicular to the film plane (Figure 2). The magnetoresistance ratio (MR) of the films was defined from $\Delta R(B, T)/R(0, T)$, where MR is the ratio between magnetoresistance difference at different magnetic field against $R(B, T)$, MR $=\Delta R(B, T)/ R(B, T) =[R(B, T)-R(0, T)]/ R(B, T)$, where $R(B, T)$ is the transverse magnetoresistance of the film at external magnetic field, B, applied perpendicular to the film plane (B) and temperature (T). Total 8 cases ($\pm I_{AC}$ and $\pm I_{BD}$ at ±B) were conducted and average MR value was obtained for one condition of the film.

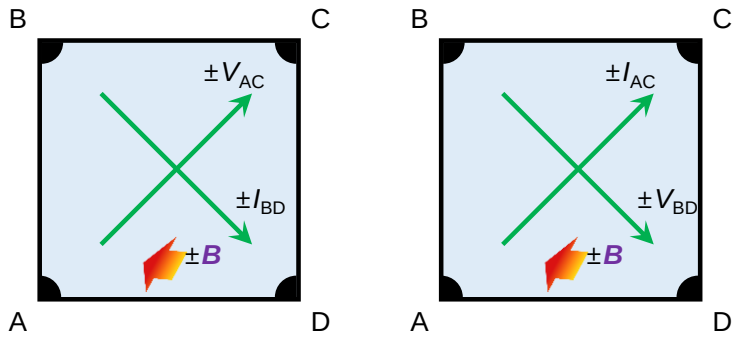

Figure 2. The transverse resistance measurement condition.

3. Results and Discussion

3.1. Qubit materials from metalophthalocyanines with pi-conjugaed ligands (MPCQ).

To maximize coherence, materials for qubits are required to pertain ordered arrangement and provide interaction between electronic spin states in qubits. In this context, metalophthalocyanines containing a magnetic ion, generally an f-block metal, could be a promising candidate[12]. In these magnets at the molecular level, the origin of the magnetism is from both orbital and spin angular momentums of a single lanthanide ion, which is placed in a ligand field. Thus challenges for robust qubits lie ahead on the combination of the f-block elements and pi-conjugated ligands, which insure optimum spin-orbit coupling combined with the crystal-field interaction with surrounding pi-conjugated ligands. A previous study showed that suitable choices of ligand field can yield a situation where the lowest substates have a large $|J_z|$ value and the energy gap between the lowest and second-lowest substates is more than a few hundred wavenumbers[13,14]. Thus we can construct a hybrid quantum materials by coupling the delocalized qubit to a qubit of matter, for example to a natural atom or to a ligand of next atom. Thus we synthesized metalophthalocyanines containing a Tb or Ln ion, as an f-block metal. Three different $Tb(Pc)_2(R)_8$ were synthesized from unsubstituted (R=H) or disubstituted 1,2-dicyanobenzene with $Tb^{3+}(acac)_3{\cdot}4H_2O$ in alcohol at elevated temperature, where the side chain (R) is H, O-alkyl, and S-alkyl. Similarly blue (anionic $[LnPc_2]^-$) and green (neutral $[LnPc_2]^0$), were obtained. The unstable anionic form was converted to the stable neutral form.

All $Tb(Pc)_2(R)_8$ were soluble and showed their characteristic optical properties. Fig 3 (a) presents the electronic absorption spectra for MPCQs to feature their characteristic Q bands. The absorption max for Q bands of $TbPC_2$ R_8 was red shifted from H to O-alkyl and further shifted in S-alkyl side chain, possibly due to the extension of the electron to the heteroatom of the side chain. The emission spectra of $TbPC_2$ R_8 were also red shifted according to the nature of side chain (R) as compared in Figure 3. Taking advantage of their solubility in organic solvent they were coated on a graphene surface and mounted on a device to examine their magnetic properties on a 2 D surface (Fig 3b and c). After coating on a graphene, the samples were washed with alcohol to remove extra molecules from the monolayer. The samples before and after washing are named as UW and W, respectively.

The magnetic resistance of the samples were determined by the Hall measurement. The magnetoresistance ratio (MR) of the films was defined from ΔR(B, T)/R(0, T), where $\Delta R(B, T)=R(B, T)-R(0, T)$, and $R(B, T)$ is the transverse resistance of the film at external magnetic field (B) applied

perpendicular to the film plane ($\perp$) and a specific temperature (T). The MR of bare graphene on quartz was ~10^{-1} range at 298 K, which had large error range in sample by sample and it was slightly decreased after depositing adlayers in ~10^{-1} range. Figure 3d shows that the $Tb(Pc_2)(SR_8)$ on graphene present the lowest resistance at both 0T and 0.53 T among the PC samples. Interestingly, it showed the highest MR as compared in Fig 3 (e). Furthermore, the washed $Tb(Pc_2)(SR_8)$ showed a higher MR to give 12.2 at room temperature, indicating that it could provide high tunability in electron spins.

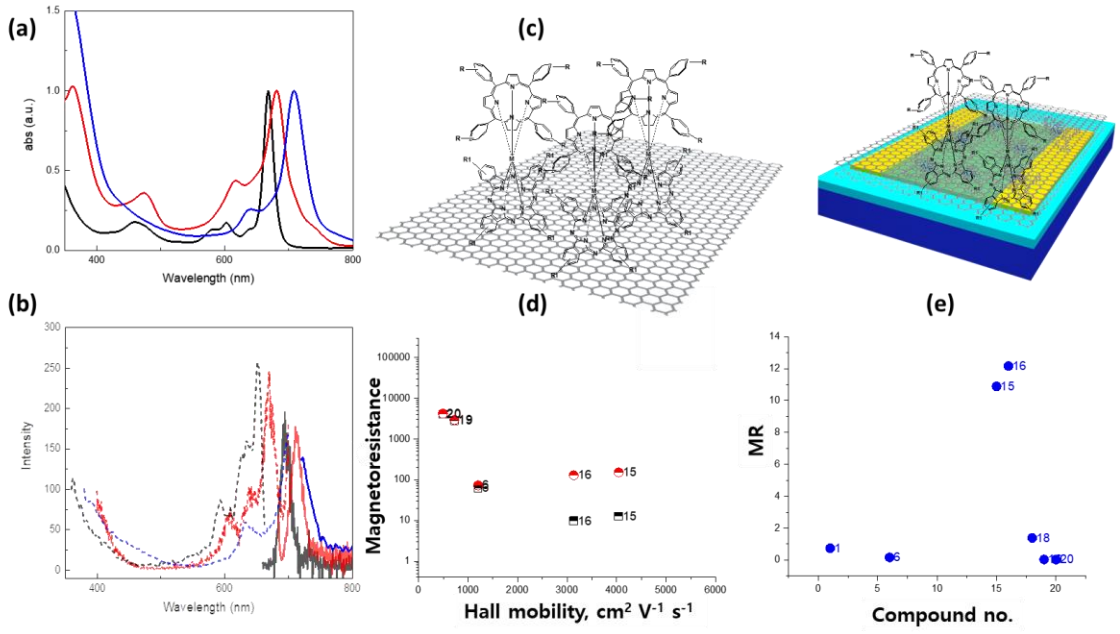

Figure 3. (a) UV and (b) photoluminescence spectra for $TbPc_2$ (black), $Tb(Pc)_2(OR)_8$ (red), and $Tb(Pc)_2(SR)_8$ (blue) in solution. (c) Arrangement of MPCQs on graphene and a device. (d) Magnetic resistance of MPCQs on graphene at 0T (black) and 0.53 T (red) as determined from Hall experiment at room temperature and (e) MR for ZnPc (6), $Tb(Pc)_2(SR)_8$ (15, UW, 16 W), and $Tb(Pc)_2(OR)_8$ (19, UW, 20 W).

3.2. Qubit materials from luminescent organic radicals (LORs)

As an organic qubit system, organic N-O radicals were explored to provide a processible soft qubits. These organic quibits could be controlled electrochemically by controlling their redox states. In particular, organic N-O radicals can be functionalized by tethering a luminescent aromatic group that are subjected to generate electron spin states through spin orbital coupling upon photopumping. Thus we synthesized luminescent organic radicals (**LORs**). To assemble these organic quibits on graphene, a linker was attached to these molecules. Putting all together we synthesized TEMPO (**T**) substituted fluorene (**Fl**) and benzothiazole (**Bt**) structures having a pyridine (**Py**) or bromo (**Br**) linker. The first structure is based on fluorene as an electron donating luminescent group, as fluorene derivative exhibited bright phosphorescence emission at room temperature. The 2nd structure is based on a benzothiazole group as an electron accepting luminescent group. These molecules are named in the order of TEMPO-luminescent group-linker as TFlPy, TFlBr, TBtPy, etc.

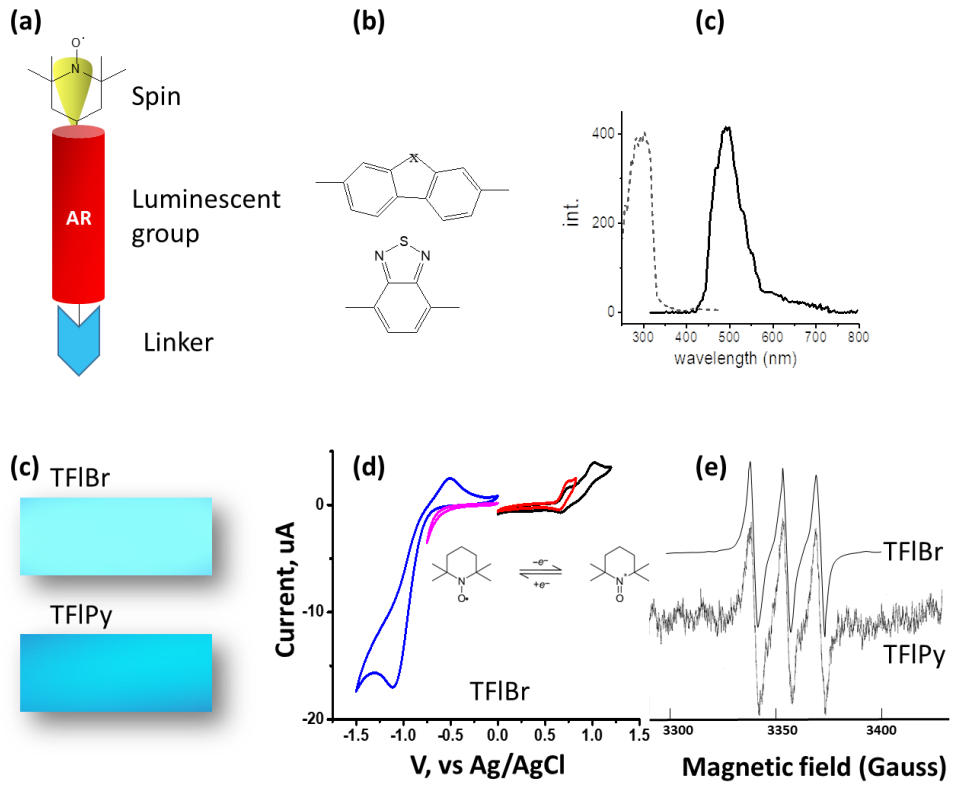

Figure 4. (a) General structure of LORs where AR units are either fluorene or benzithiazol group. (b) Absorption (dashed) and phosphorescence of TFlBr at room teerature. (c) Photogrps for the emission of TFlBr and TFIPy. (d) Cyclic voltammograms for TFlBr (black and blue) and TEMPO (red and magenta) in a there electrode system. (e) ESR spectra for TFlBr and TFlPy.

The Fl derivatives (TFlBr, X= CH_2 and $C(alkyl)_2$) exhibited phosphorescence emission maximized at 500 nm in solution at 298 K (Fig 4 b) but decayed fast. When these Fl derivative was incorporated into a poly(methyl methacrylate) film, the phosphorescence was similarly observed even under air at room temperature for over several days. TFlPy also showed phosphorescence emission with green blue color as compared in Fig 4 c. The Bt derivative showed fluorescence in both solution and film. The CV for TFlBr in solution showed characteric redox peaks, arising from TEMPO unit, indicating that the carrier density of these organic radical derivatives could be controlled electrochemically. All the Fl and Bt derivatives showed the presence of radical from their ESR spectra as shown for TFlBr and TFlPy in Fig 4 e. The monolayers of these radicals were doped on the graphene surface via solution process, to determine their magnetic properties. TO explore the effect of molecular alignment on the MR, a self-assembled host, 1,3,5-tris(3,5-bis(dodecyloxy)styryl)benzene (**TSB12**) was first coated and then the solution of LORs were coated on the templated coated graphene. The luminescent organic radicals showed poor MR when the molecules were coated without the TSB template. However it became large and the TBtPy monolayer showed a high magnetic resistance ratio of 1.6.

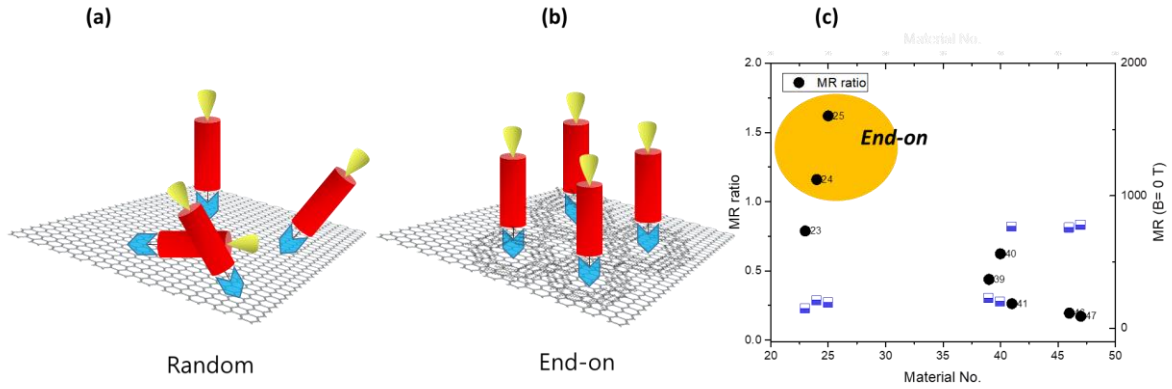

Figure 5. (a) Random arrangements of LORs on a graphene surface without a self-assembled host (a). (b)End-on arrangement of LORs on a **self-assembled host** that were pre-assembled on a graphene surface before LOR coating. (c) MR (black) and magnetoresistance at 0 T (blue)for LORs synthesized in this study and magnetoresistance.

While LORs may provide optical teleportation of spins, it could be possible to tune their spin states by electronically, ustilizing electrochemically active polymer channels. As an electrically active organic qubit system, polaronic radicals of conjugated polymers were explored to provide a processible soft qubits. These conjugated polymers are particularly interested for their processibility as a film and easy synthesis. On the other hands, the structural ordering is challenging due to their intrinsic entagled structure due to random polymerization. Thus we explored a method to integrate the polymeric quantum units by solution processing of the molecule and explore the controllability of magnetic resistance by electrical stimuli

3.3. Qubit materials from electroctive Conductive Polymers and their Giant Magneto-Thermoelectric Effect

Conductive polymers (CPs) have drawn significant attention of an urgent need for low-cost, transparent, wearable, solution processable and environmentally benign demands for its potential applications as human integrated devices, and healthcare biosensors.[15, 16] Among the conducting polymers, poly(3,4-ethylenedioxythiophene)s (PEDOTs) were explored for polymeric qubits. To force them at end-on orientation, a pyridine functionalized EDOT ligand (**EDOT-Py**) was synthesized, in which the nitrogen atom is used for binding to a self-assembled Zinc phthalocyanine (ZnPc) or graphene. The coordination of ZnPc to the ligand EDOT-Py was confirmed by UV-Vis spectroscopy, which showed absorption maximum peak shift of ZnPc in toluene (coordinating free) during increasing addition of EDOT-Py.

The surface-confined host-guest approach was performed by two step processes on graphene.[7] First, the 2D nanoporous honeycomb network template (host) was prepared on graphene surface by the exquisitely designed self-assembly of TSB12 (G1). Then, the ZnPc:EDOT-Py complex (guest) immobilized into the hexagonal nanopore array (G3). PEDOT was grown by solution casting polymerization method on the surface functionalized graphene Hall measurement was performed to study the magnetoresistance effect of PEDOT films polymerized on surface functionalized graphene at an ambient condition . For the graphene applied films, the Hall mobility was highly increased and the Hall voltage signal was very stable for measurement cycles. Interestingly, the end-on structured PEDOT (PG3) showed higher Hall

mobility of 701 cm^{-2} V^{-1} s^{-1} with a high σ (1690 S cm^{-1}). This result could coincide with the effect from orientation of PEDOT:Tos chain. The polymer backbone in end-on orientation can be more affected by a Lorentz force induced from an external magnetic field which is perpendicular to the film than that of edge-on orientation because carriers can strongly transport through *b*-axis direction which is the major packing for the former than *a*-axis direction in major packing for the latter.[17]

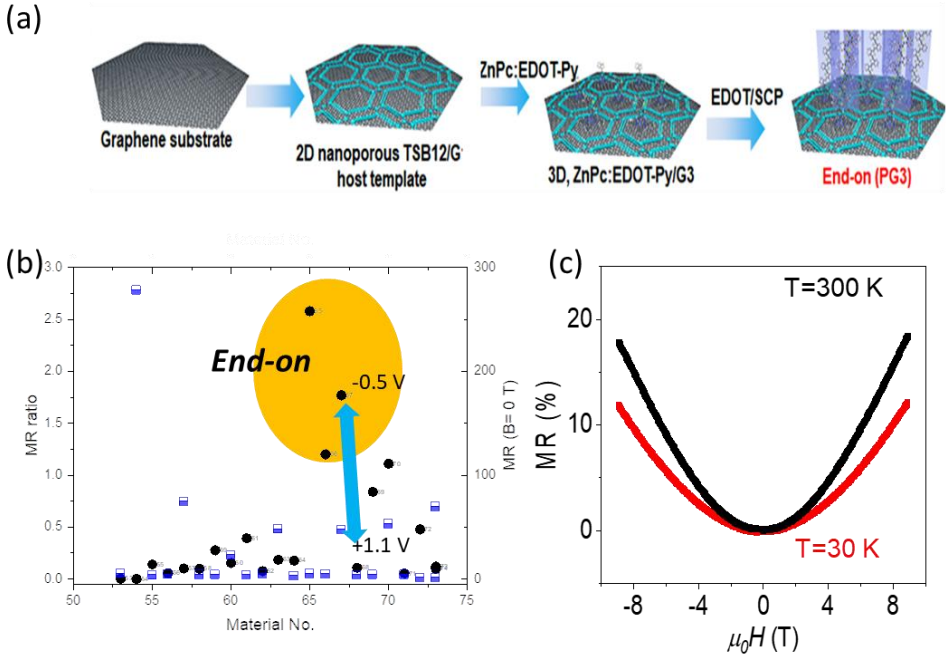

Figure 6. (a) End-on arrangement of PEDOTs on a self-assembled host that were pre-assembled on a graphene surface before EDOT coating. (b) MR (black) and magnetoresistance at 0 T (blue)for PEDOTs synthesized in this study. (c) PPMS results for the end-on structure PG3 sample at 300K and 30K, respectively.

For a profound understanding of the charge carrier transport, thermoelectric measurement was examined and Seebeck coefficient (*S*) was analyzed with the Hall parameters. *S* values were consistent in the range of 82.6-89.9 μV K^{-1}. The PEDOT:Tos films were polymerized on the surface functionalized graphene which could affect the phonon transport and carrier mobility of the film. Hall measurement was further analyzed to study the magnetoresistance effect of PEDOT films polymerized on surface functionalized graphene at an ambient condition. The MR of bare graphene on quartz was ~10^{-1} range at 298 K, which had large error range in sample by sample. However, this error range was reduced after coating the PEDOT:Tos film on (surface functionalized) graphene surface. The MR of PEDOT film without end-on orientation was generally lower than 1 at 298 K, which means that the PEDOT:Tos film has a small magnetic response under room temperature condition (Fig 6b). This value was dramatically increased in PG3, showing a high MR of 2.58. This is ~258 times higher value than the reported MR of PEDOT:PSS[21] .

Physical property measurement system (PPMS) was further performed to study the MR effect and carrier transport phenomenon of PEDOT films at a high magnetic field up to 9 T and a low temperature (30 K). PG3 showed a symmetric parabolic MR response at ±9 T and 300 K (Figure 6c). This MR effect was dramatically decreased by reducing temperature to 30 K,. Normally, the

negative MR phenomenon is interpreted as weak localization effect while the electron-electron interaction results in positive MR.[20, 22] Therefore, the two effects can coexist in the MR response which result in the negative or positive signs when varying the temperature. The negative MR for the CPs from the weak localization effect was reported at in the literature.[52-54] The anisotropic effect is originated from a two-dimensional transport of thin film. In percolation system, polaron and bipolaron in film can be largely affected by MR mechanism. In addition, this MR value was similar to the MR of single layer graphene (~400% at 1.9 K)[55] and is one of the largest value than that of other conductive polymer films.

We determined the change of S in B ($\partial S/\partial B$), magneto-Seebeck (MS) effect, in the thermovoltage measurement setup.[19] The $B_{\perp}$ was varied from ~0 to 300 mT using a 25 mT/30 s step increase and decrease cycles. When the $B_{\perp}$ (300 mT) was applied, PG3 showed a large decrease of S, 51%. When the B (224 mT) was parallel to the film plane (//), the PG3 film exhibited 12% decreased S value. The $\partial S/\partial B_{\perp}$ and $\partial S/\partial B_{//}$ were -142, μV/KT and -43 μV/KT for PG3, respectively. These S variation under B was larger than the Ni nanowires.[19] These large change may derived from the conductance change of DoS near the E_F.[4, 21] From the Hall effect, Lorentz force applied to a backward direction oriented parallel to the thermoelectric carrier movement, which enhances the magneto-thermoelectric response of the PG films. Finally, a large magneto-thermoelectric (MTE) effect was derived from the MR and MS effect (Figure 7b and c). By switching the small $B_{\perp}$ of 200 mT to the films, PG3 showed the highest MTE of ~-73.6% at 298 K which was much higher value than the reported PEDOT:PSS film which had a magneto-PF of -3.8% at room temperature.[21]

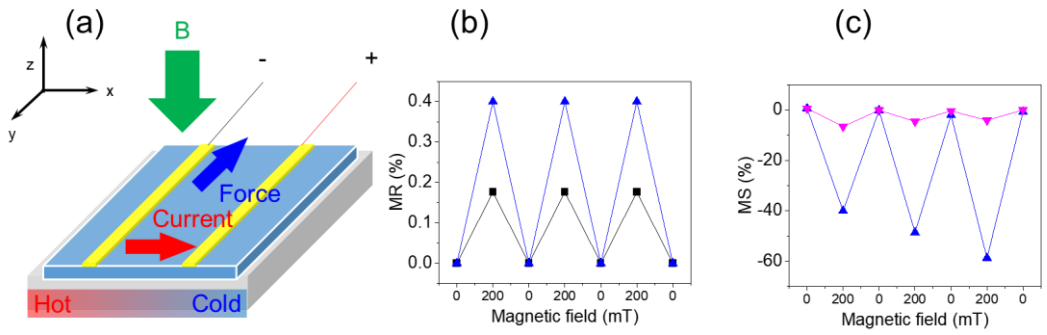

Figure 7. (a) A schematic diagram for magneto-thermoelectric device. (b) Magnetic Switchability of the end-on PEDOT (PG3, blue) against random PEDOT (black) on graphene (c) magneto-thermoelectric Seebeck response of the PG (blue) and random oriented PEDOT (magenta) on graphene at room temperature.

3.4. Non-covalently Tethered Qubits (NCTQ)

Non-covalent self-assembly of polyaromatic molecules on graphene allows generation of precise arrays of molecules and materials [8]. The highly selective and specific interaction between polyaromatic moieties and graphene surface could be exploited to achieve highly

ordered arrangement of qubits. The approach is summarized in Figure 8(a-b). The ligand can be divided into three parts, first the pyrene tether, second a spacer groups whose rigidity as well as optical chirality can be controlled synthetically and the third moiety which complexes with relevant metal atoms. Molecular level assemblies of non-covalent molecules on graphene surfaces have been studied by many groups. This proposal will take insights from the literature in trying to create a uniform array of qubits. Further laser induced graphene oxidation[18] can be used to create patterned graphene surfaces oxidized and non-oxidized regions as seen in Figure 10(c-d). These regions can then be used to define delocalization of non-covalently assembled qubits. If successful, these approaches could be extended to transition metal dichalcogenide (TMDC) 2D materials.

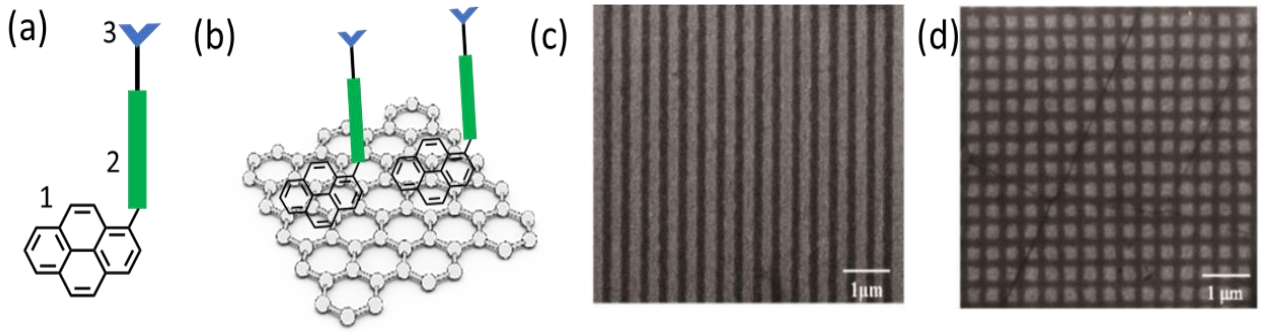

Figure 8. Non-covalent assembly of ligands capable of complexing with magnetically suitable ions on graphene.

Vanadium (IV) with its large nuclear spin and relatively low electron spin is characterized by improved coherence due to inhibition of spin related decoherence pathways. To demonstrate non-covalently assembled vanadium complexes on graphene sheets, we designed a ligand (L1) capable of forming complexes with vanadium while also being able to couple to the surface of graphene. The ligand L1 featured a pyrene moiety at one end acting as an anchor group capable of associating with the graphene surface through non-covalent interactions. The other end contained a catechol residue which was capable of complexing with vanadium. The ligand L1 was synthesized following the procedure in Figure 1. The synthesis of the ligand was confirmed by ^{1}H -NMR spectroscopy which showed aromatic peaks corresponding to the fused aromatic groups of the pyrene as well as the four aromatic carbons associated with the catechol moiety (Figure 9-10).

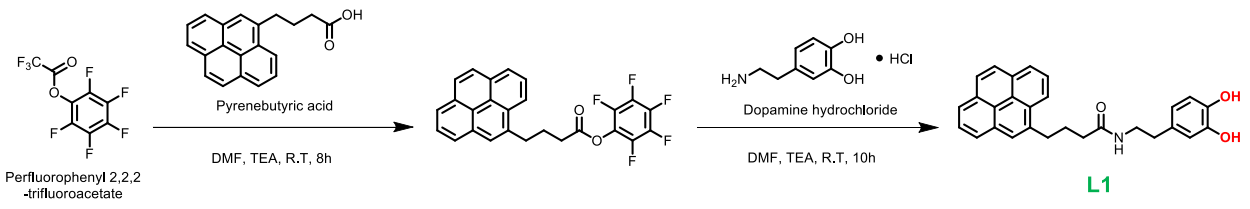

Figure 9. Synthesis of hydroxyl ligand (L1).

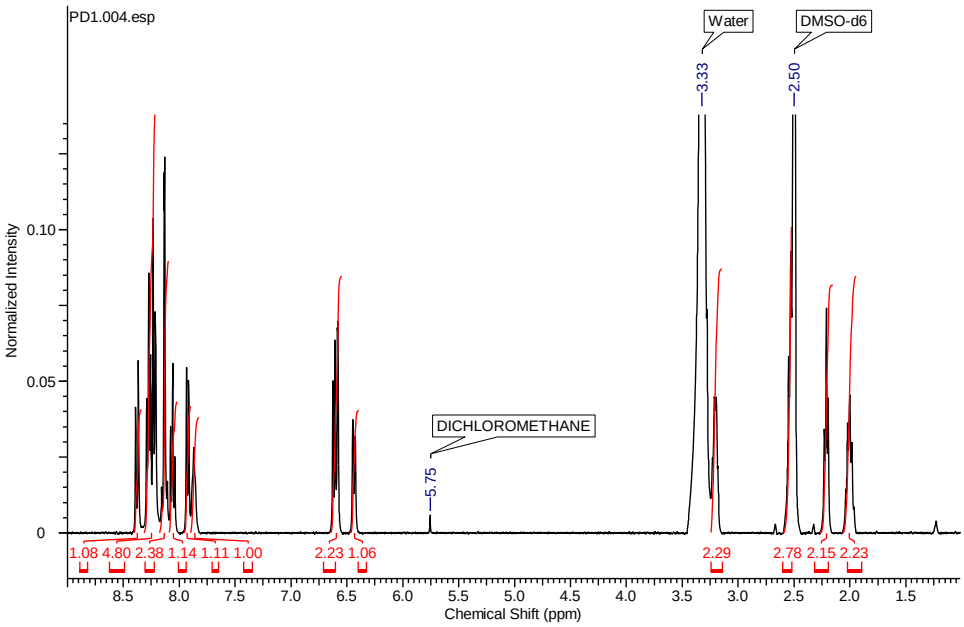

Figure 10. ^{1}H NMR (400 MHz) spectra of hydroxyl ligand (L1) in DMSO.

The vanadium(IV)-L1 complex VL1 was synthesized using the procedure elaborated in the experimental section, the synthesis scheme can be seen in Figure 11. The formation of the blue colored complex was confirmed visually through the color change of the reaction mixture and spectroscopically with UV-Vis and PL spectroscopy. The complex VL1 showed UV and PL characteristics like that of the pristine ligand L1. Typical pyrene peak was seen in the UV-Vis spectra of L1 and VL1. These spectra were also compared to pyrenebutanoic acid, and the vanadium precursor vanadyl acetylacetonate ($VO(acac)_2$). The characteristic optical absorption of the latter was found to be in sharp contrast to all pyrene containing molecules. The same trend was repeated in the PL spectra of these compounds (Figure 12). The vanadium precursor did not give any peak, while the rest of the three compounds did. The UV pyrene peaks appeared at 342 nm, 326 nm, 313 nm, 276 nm, and 265 nm. PL peaks showed at same positions of 417, 396, and 378 nm due to pyrene group for pyrenebutanoic acid, L1, and VL1.

There were subtle differences between the IR spectra of L1 and VL1. The IR spectrum can be seen in Figure 13. The main differences were seen in the region between 2700 cm^{-1} and 4000cm^{-1} constituting the -CH, -OH and -NH stretch peaks. The sharp amide -NH stretch vibration in L1 at 3342 cm^{-1} was observed after complex formation. While the -OH peaks, 3444 cm^{-1} in L1 was appeared in VL1. We should consider the spatial nature of and bonds in the complex when interpreting the IR spectra. The hydrogen bonding interaction with the tertiary butyl nitrogen also plays into the differences in -OH stretch energies seen between L1 and VL1. The aromatic -CH stretch of both L1 and VL1 remains unchanged.

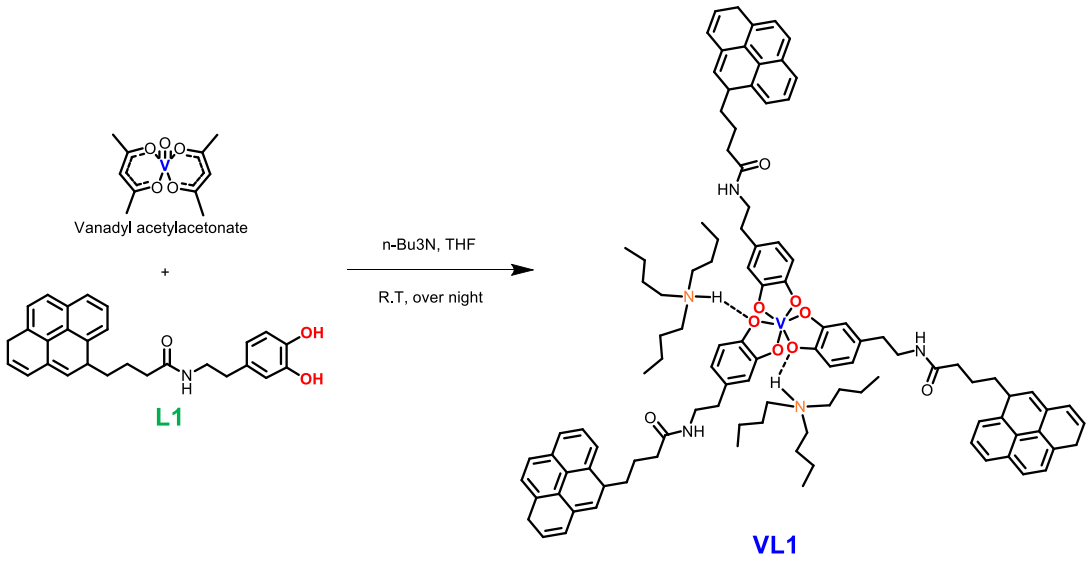

Figure 11. Synthetic scheme of vanadium hydroxyl ligand complex (VL1).

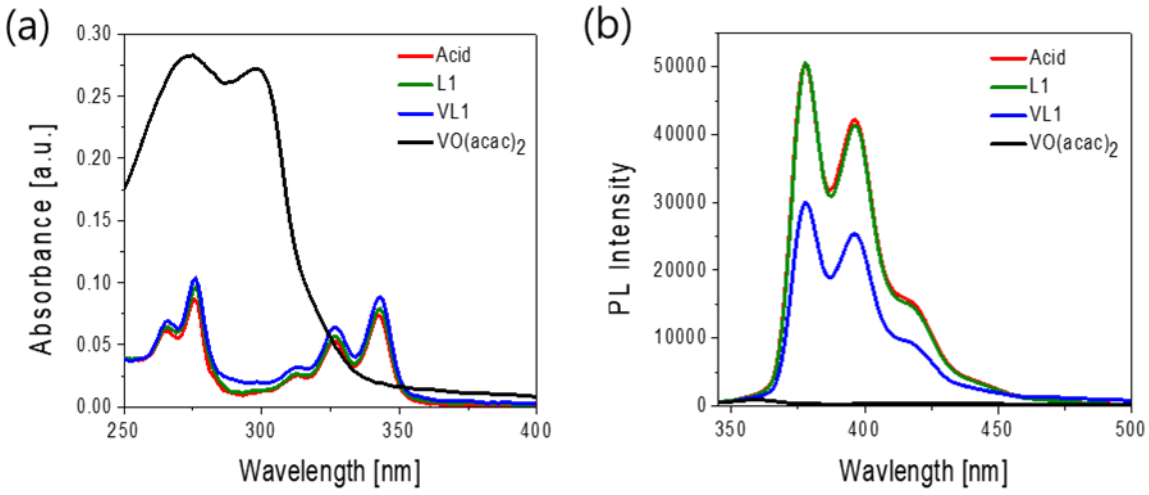

Figure12. (a) UV-visible spectra in solution (THF) (b) PL-spectra in solution (THF) of Pyrene butyric acid, L1, VL1 and $VO(acac)_2$ **.**

The complex VL1 ligand was coupled to graphene for simple ultrasonication experiments, which were carried out under room temperature. The functionalization was spectroscopically followed by UV spectra. A graphic depicting synthetic process can be seen in Figure 14. The UV and PL of L1, VL1, graphene, and GVL1 are compared in Figure 15. The relative ratio of graphene:VL1 was varied to see the extent of functionalization of the graphene sheets with VL1. Two GVL1 samples were prepared, namely, GVL1A and GVL1B, where the Graphene : VL1 weight ratio were 1:1 and 1:5, respectively. The graphene characteristics were prominent in the absorption spectrum in the case of GVL1A with lower concentration of VL1. Pyrene peaks were more visible in GVL1B due to increased concentration of pyrene. We can conclude that both GVL1A and GVL1B contain pyrene to a different extent. We are currently working on time-dependent measurement of the fluorescence of these nanohybrids.

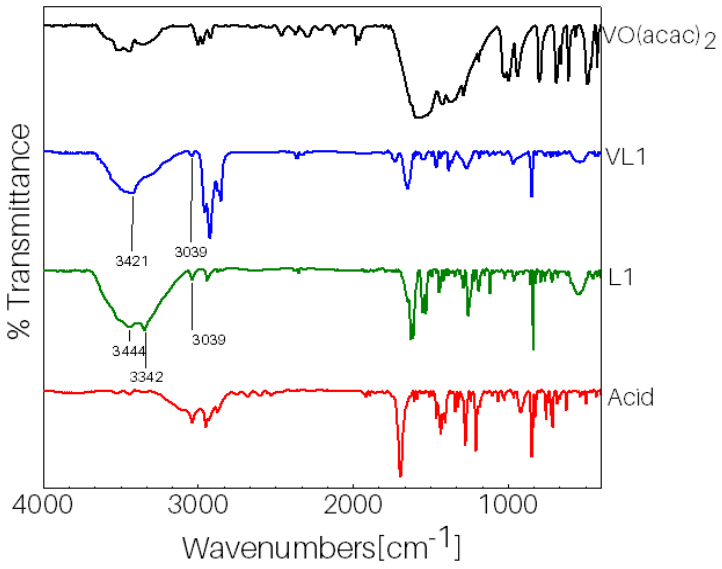

Figure 13. FT-IR spectrum of pyrene butyric acid, L1, VL1, $VO(acac)_2$.

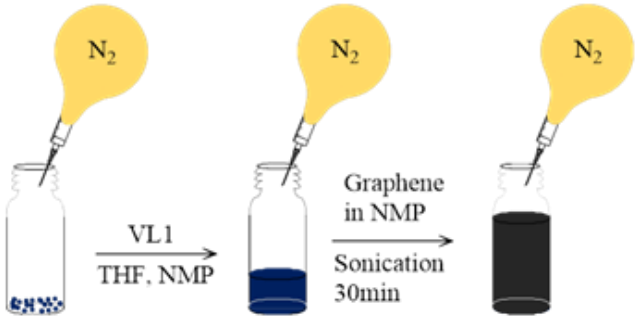

Figure 14. Synthetic route of GVL1.

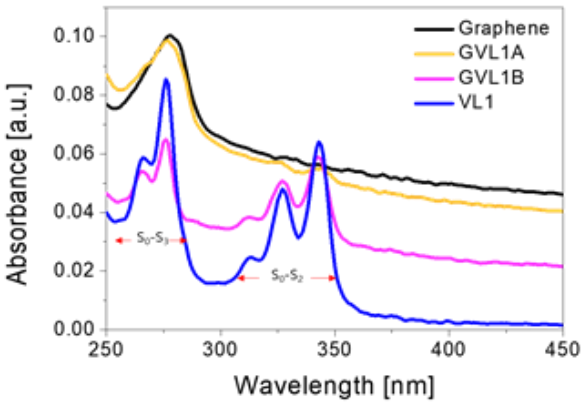

Figure 15. (a) UV-visible spectra in solution (THF) (b) PL-spectra in solution (THF) of Graphene, GVL1A, GVL1B and VL1. (GVL1A is graphene:VL1 = 1:1, GVL1B is graphene: VL1 = 1:5).

We had also designed a ligand L2 for coupling magnetically interesting nanoparticles to the

graphene surface. The ligand L2 contained a bithiolane moiety at one end and a pyrene moiety at the other. The bithiolan end is suitable for associating with different nanoparticles. We had a problem while synthesizing the bitholane ligand L2 in Figure 16. While checking the synthesis process and progress by TLC, it was confirmed that there were substances different from those expected to be L2, and it was not easy to separate the two substances. The other substances are either a material that has a charge generated by the coupling of DMAP and DCC, or the S-S bond of lipoic acid can be easily broken, so it seems that it is a substance synthesized as L2 with an S-H bond in a ring open state or decomposed. Therefore, we will synthesize L2 by designing a different scheme given in Figure 15.

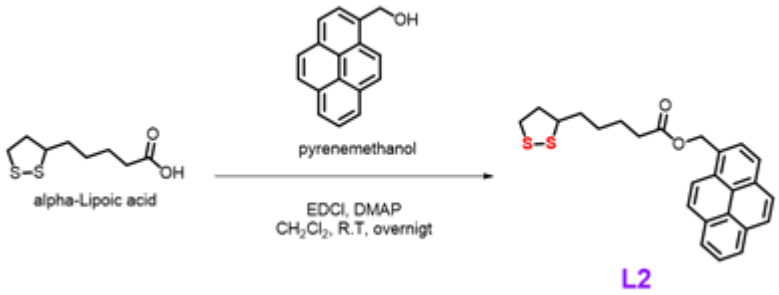

Figure 16. Synthesis of the bitholane ligand L2.

4. Conclusions and Outlook

Within a year of research work, we explored a strategy to design organically modified qubits (**OMQs**) starting from metalophthalocyanines containing lanthanide ions. As the origin of the magnetism could be from both orbital and spin angular momentums of these crystals, they were designed to pertain ordered arrangement of spins by substituting ligands with a long chain. To explore the controllability of electronic spins at organic units, luminescent organic radicals (**LORs**), and conjugated polymer magnets were designed. These OMQs were oriented vertically on a 2D surface, having spins at end, to modulate electronic properties of the surface against the spin direction. The ligand on the metalophthalocyanines was critical to achieve a large magneto resistance ratio (MR). Thus a thioalkyl ligand of the $Tb(Pc)_2(SR)_8$ showed the highest MR at room temperature among the $Tb(Pc)_2(R)_8$, indicating that it could provide high tunability in electron spins. The end-on structured LORs showed large MR, which is much larger than those of the reported materials. The end-on oriented PEDOTs on graphene showed a high degree of crystallinity and free-electron-like charge transport properties with an enhanced Hall mobility, which allowed modulation of phonon transfer via external stimuli. Taking advantage of graphene functionality, thermoelectric properties were largely modulated *via* external magnetic field as a giant magneto-thermoelectric effect of ~-73.6% and Seebeck coefficient of -49% at 298 K. This result provides a unique tool for a multifunctional electron spintronics. Thus further research on robust qubits based on OMQs should provide optimum spin-orbit coupling for spin entanglement and tunability of their electro-optical teleportation. To develop non-covalently tethered qubits with vanadyl derivatives, VL1 was synthesized. The MR properties and the single crystal XRD measurements of VL1 will be carried out to confirm the structure of the complex. We have confirmed the synthesis of both GVL1A and GVL1B, we will use characterization techniques like SAXS or AFM/STM measurements to confirm their nanoscopic structure. Electron paramagnetic resonance (EPR) spectroscopy of both VL1 and

GVL1 nanohybrids will be carried out to measure the coherence lifetime and confirm the magnitude of the hyperfine interactions. Such an evaluation will reveal the real potential of the developed materials for QIP.

5. Publications (Acknowledged Office of Scientific Research (AFOSR) under the grant number FA9550-19-S-0003)

1). Rémond, M., Hwang, J., Kim, J., Kim, S., Kim, D., Bucher, C., Bretonnière, Y., Andraud, C., Kim, E., "Push–Pull Dyes for Yellow to NIR Emitting Electrochemical Cells", Adv. Funct. Mater. 2020, 2004831.

2). Kim, H. J., Kim, B. , Auh, Y., Kim, E. "Conjugated Organic Photothermal Films for Spatio-temporal Thermal Engineering", Adv. Mater. 2021, 33, 2005940.

3). Kim, B., Cho, C., Han, M., Attias, A., Kim, E. "Giant Magneto-Thermoelectric Effect of Conductive Polymer/Graphene Films from Self-Assembled 3D Tecton", Adv. Funct. Mater. 2021, 31, 45, 2105297

4). Cho, C., K. Chang, Kim, B., Kim, E. "Tunability of Magnetoresistance for End-on Assembled Organic Radicals at Room Temperature, in preparation.

5). K. Chang, Cho, C., Kim, E. "Side chain induced Magnetoresistance in terbium phthalocyanines, in preparation.

6). Hong, S.-J., Hwang, D-Y.., Prabhakaran. P., Lee, K.-S., "Graphene Heterostructures Containing Immobilized Vanadium Complexes for Quantum Bits", in preparation, 2020.

6. References

1 Arute, F., Arya, K., Babbush, R., Bacon, D., Bardin, J. C., Barends, R., Biswas, R., Boixo, S., Brandao, F. G., Buell, D. A., Quantum supremacy using a programmable superconducting processor. *Nature* **574**, 505-510 (2019).

2 Arvidsson-Shukur, D. R. M., Yunger Halpern, N., Lepage, H. V., Lasek, A. A., Barnes, C. H. W., Lloyd, S., Quantum advantage in postselected metrology. *Nature Commun.* **11**, 3775, doi:10.1038/s41467-020-17559-w (2020).

3 Fulton, S. *What Happened to Quantum Supremacy? Quantum Computing Needs a New Success Metric*, <https://www.zdnet.com/article/what-happened-to-quantum-supremacy-quantum-computing-needs-a-new-success-metric/> (2020).

4 Cavaliere, F., Mattsson, J., Smeets, B., The security implications of quantum cryptography and quantum computing. *Network Security* **2020**, 9-15 (2020).

5 (a) Schleich, W. P., Quantum physics: Engineering decoherence. *Nature* **2000,** *403* (6767), 256; (b) Takahashi, S.; Tupitsyn, I.; Van Tol, J.; Beedle, C.; Hendrickson, D.; Stamp, P., Decoherence in crystals of quantum molecular magnets. *Nature* **2011,** *476* (7358), 76.

6 Morello, A.; Stamp, P.; Tupitsyn, I. S., Pairwise decoherence in coupled spin qubit networks. *Phys. Rev. Lett.* **2006,** *97* (20), 207206.

7 Sosa-Vargas, L., Kim, E., Attias, A.-J., Beyond "decorative" 2D supramolecular self-assembly: strategies towards functional surfaces for nanotechnology. *Materials Horizons* **4**, 570-583 (2017).
8 Zadrozny, J. M., Niklas, J., Poluektov, O. G., Freedman, D. E., Multiple quantum coherences from hyperfine transitions in a vanadium (IV) complex. *J. Am. Chem. Soc.* **136**, 15841-15844 (2014).
9 Parvez, K., Wu, Z.S., Li, R., Liu, X., Graf, R., Feng, X., Müllen, K., Exfoliation of graphite into graphene in aqueous solutions of inorganic salts. *J. Am. Chem. Soc.* **136**, 6083–6091 (2014).
10 Kim, B.; Han, M.; Kim, E., Photothermally powered conductive films for absorber-free solar thermoelectric harvesting. *Journal of Materials Chemistry A* **2019,** *7* (5), 2066-2074.
11 Cho, B.; Park, K. S.; Baek, J.; Oh, H. S.; Koo Lee, Y.-E.; Sung, M. M., Single-Crystal Poly(3,4-ethylenedioxythiophene) Nanowires with Ultrahigh Conductivity. *Nano Lett.* **2014,** *14* (6), 3321-3327.
12 Cardona-Serra, S.; Clemente-Juan, J.; Coronado, E.; Gaita-Ariño, A.; Camón, A.; Evangelisti, M.; Luis, F.; Martínez-Pérez, M.; Sesé, J., Lanthanoid single-ion magnets based on polyoxometalates with a 5-fold symmetry: the series $[LnP_5W_{30}O_{110}]^{12-}$($Ln^{3+}$ = Tb, Dy, Ho, Er, Tm, and Yb). *J. Am. Chem. Soc.*, **2012,** *134* (36), 14982-14990.
13 Jenkins, M. D.; Naether, U.; Ciria, M.; Sesé, J.; Atkinson, J.; Sánchez-Azqueta, C.; Barco, E. d.; Majer, J.; Zueco, D.; Luis, F., Nanoscale constrictions in superconducting coplanar waveguide resonators. *Appl. Phys. Lett.* **2014,** *105* (16), 162601.
14 Jenkins, M.; Hümmer, T.; Martínez-Pérez, M. J.; García-Ripoll, J.; Zueco, D.; Luis, F., Coupling single-molecule magnets to quantum circuits. *New J. Phys.* **2013,** *15* (9), 095007.
15 Park, T.; Na, J.; Kim, B.; Kim, Y.; Shin, H.; Kim, E., Photothermally Activated Pyro electric Polymer Films for Harvesting of Solar Heat with a Hybrid Energy Cell Structure. *Acs Nano* **2015,** *9* (12), 11830-11839.
16 Chen, S.; Kang, E. S. H.; Shiran Chaharsoughi, M.; Stanishev, V.; Kühne, P.; Sun, H.; Wang, C.; Fahlman, M.; Fabiano, S.; Darakchieva, V.; Jonsson, M. P., Conductive polymer nanoantennas for dynamic organic plasmonics. *Nature Nanotechnology* **2020,** *15* (1), 35-40.
17 Noriega, R.; Rivnay, J.; Vandewal, K.; Koch, F. P. V.; Stingelin, N.; Smith, P.; Toney, M. F.; Salleo, A., A general relationship between disorder, aggregation and charge transport in conjugated polymers. *Nat. Mater.* **2013,** *12* (11), 1038-1044.
18 Xu, X.; Shi, B.; Zhang, X.; Liu, Y.; Cai, W.; Ren, M.; Jiang, X.; Rupp, R. A.; Wu, Q.; Xu, J., Laser direct writing of graphene nanostructures beyond the diffraction limit by graphene oxidation. *Opt. Express* **2018,** *26* (16), 20726-20734.